

Heat Load Patterns on Tore Supra ICRH Antennas.

L. Colas , M. Bécoulet, L. Costanzo, S. Pécoul⁺, S. Heuraux⁺,
S. Brémond, C. Desgranges, A. Bécoulet, Ph. Ghendrih

*Association Euratom - CEA pour la Fusion Contrôlée
CEA Cadarache - 13108 S^t Paul les Durance – France*

⁺*LPMI, Unité du CNRS 7040, Université Henri Poincaré, Nancy 1
BP 239, 54506 Vandœuvre Cedex, France*

With its upgrade CIEL, Tore Supra aims at demonstrating a heat removal capability of 15MW convected and 10MW radiated, over typically 1000s. Most of the heating power will be delivered by Radio-Frequency (RF) systems, including Ion Cyclotron Resonance Heating (ICRH). It is thus crucial to ensure that the RF launching structures themselves are able to sustain, in steady state regime, high thermal loads from the plasma.

In earlier systematic monitoring with infrared cameras, several ICRF antenna-plasma interaction phenomena could be identified on Tore Supra [1]. The present paper focuses on a non-resonant RF-induced process, hardly avoidable and potentially harmful to the antenna. The parametric dependencies of the phenomenon, and especially the role of the local density, are studied experimentally in Ergodic Divertor (ED) discharges, using visible light films and Langmuir probes. A first interpretation of the heat load distribution is then presented, in the framework of RF-sheath physics [2-3]. Numerical simulations of potential rectification near ICRF antennas, in realistic geometry, investigate the role of particle redistribution by RF-induced $\mathbf{E} \times \mathbf{B}$ convection to explain the observed up-down asymmetries of the hot spots.

1. Antenna thermal behavior in Ergodic Divertor plasma edge.

From a large database of plasma shots in limiter configuration, the local RF field, the local density in front of the antennas (although not measured), and geometrical factors, were suspected to be relevant parameters influencing the hot spot intensity [1]. A similar study was performed with ED discharges. ICRF antenna Q5 (named after its position on horizontal port 5 of Tore Supra) was monitored by a dedicated visible light camera located on a nearby port. It provides one image every 40ms, with a space resolution better than one millimeter. Visible light was turned into CCD images, and digitized for offline analysis. Because the final signal was not calibrated and could saturate, the absolute radiation intensity could not be recovered. However, relative comparisons were possible between nearby shots. We focused our attention on a small region near the lower-left corner of the Faraday screen (FS), where the thermal radiation from hot zones could clearly be separated from the background plasma light.

The effect of the local RF field (see ref. 1) could be reproduced in the ED experiments : the corner zone only lights-up when the observed antenna is energized, whatever other additional power. The hot spot is all the more intense as the local power is high. ED plasmas are especially helpful to test the role of the local density in the plasma antenna interaction. First, the edge density can be recorded by a set of domed Langmuir probes fixed on ED modules. We privileged probe D5, that was always magnetically connected to antenna Q5, and was thus best representative of the density close to that object. It was checked, over 19 shots and various ED density regimes, that the measurements on D5 are well correlated with the ICRF coupling resistance, which is another indicator of the density profile in the vicinity

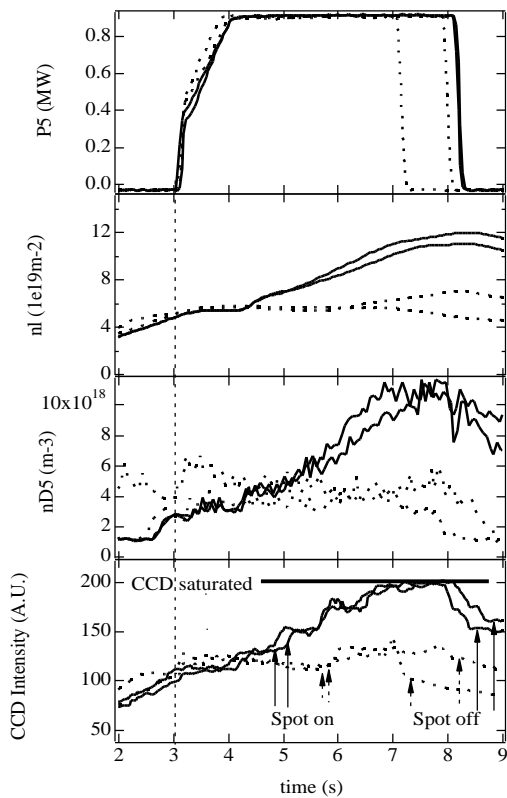


Fig. 1 : change of core density n_i .

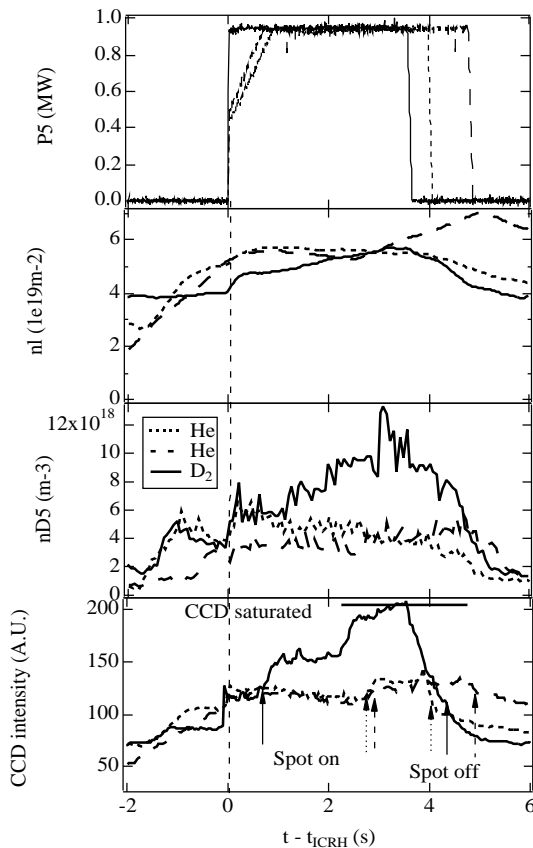


Fig. 2 : He vs D_2 fuelling gas.

of antenna Q5. ED plasmas also offer a wide variety of edge density regimes [4]. The ED magnetic perturbation creates a complex flux tube pattern at the plasma edge, consisting of field lines connecting the plasma facing components to the inner plasma shells over short parallel distances. In this zone, parallel transport, as well as atomic physics (ionization, charge exchange) are dominant. As a first consequence, the edge density is more sensitive than in limiter configuration to small changes of the chord integrated density n_i , used for core density feedback. Moreover, the edge density also depends on other parameters such as : the working gas, the position of the moveable Outboard Pumped Limiter (OPL) in the ergodic zone and, to a smaller extent, additional power.

This provided three different means to change the local density, from shot to shot : 1. scanning n_i ; 2. Comparing shots with similar n_i with He and D_2 fuelling gases ; or 3. inserting the OPL close to the plasma separatrix. The time traces of these experiments are presented on figures 1-3, leading to a common observation : the higher the edge density, the earlier the hot spot appears and/or the more intense it gets in its final regime. This comforts the local density near antennas as a key parameter governing the hot spots physics.

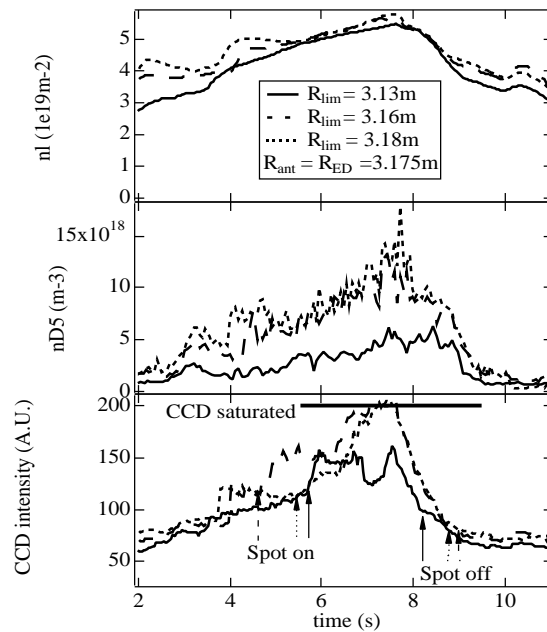


Fig. 3 : OPL insertion into the ergodic zone.

2. Heat load asymmetries and density distribution

In limiter plasmas, most of the hot zones on IR films, and most reported damages, are located on the lower part of the FS structure [1]. This result is counter-intuitive since it does not preserve the geometrical symmetry of the experimental setup with respect to the antenna center. A partial shadowing of the FS by nearby objects, or a bad mechanical positioning of the antenna in the vacuum vessel, are unlikely explanations for the asymmetry, since similar observations were made for 3 ICRF couplers, i.e. for 3 different toroidal locations.

In this section another interpretation is put forward, in the context of RF-sheath physics. Plasma potential rectification by RF-sheaths [2] is the leading explanation for the observed hot spots [1]. At constant temperature, the ion heat flux across the sheath is proportional to the local density and to the rectified potential. While a symmetry of the potential is expected from that of the antenna, density asymmetries can be envisaged. Indeed, intense localized gradients of the potential arise around the antenna. $\mathbf{E} \times \mathbf{B}$ particle transport sets-in, braking the symmetry and changing the density map. Density profile modifications in front of powered antennas, measured experimentally [5-6], were already attributed to that mechanism [3]. Assuming that the DC electric field points radially inward, convective cells on Tore Supra flow from the top to the bottom of the antenna, i.e. density depletion is expected in the upper part, and over-density at the lower. For more quantitative insight, the phenomenon was simulated numerically, in realistic geometry. In the spirit of ref. [8], a 3-step procedure was followed :

1°) A 3D mapping of the RF near field was computed self-consistently with the ICANT code [7]. A complex metallic structure was introduced, including two straps, a thick antenna box, a Faraday screen with tilted bars, a septum and two lateral bumpers. In order to achieve the required spatial resolution of a few cm for the map, the RF field wavenumber spectrum was calculated up to $k_{\parallel} = \pm 450/R$ and $k_{\text{pot}} = \pm 150/a$. Although the simulated space domain was in the vacuum, the presence of an inhomogeneous plasma at the boundary was accounted for by a spectral impedance matrix, obtained by the BRAFFA code. In the present state of ICANT, only the Fast Wave was retained in the plasma, and the DC magnetic field was in the toroidal direction. The RF electric field was normalized to 1MW ICRF power coupled to the plasma.

2°) The magnetic structure in front of the antenna was determined. Two field-line tracing codes were available, one for the real antenna with the complete Tore Supra magnetic field, the other one for the simpler magnetic topology (straight lines in a plane) and the flat antenna structure and in ICANT. Comparison of the two codes was used to adjust the radial structure of the ICANT antenna, so as to approximate with the simplified setup the magnetic connection pattern obtained for the real antenna. A 2-D RF potential map was computed by integrating the RF parallel electric field along the open field lines determined previously.

3°) This map was introduced into a 2D fluid code : CELLS. Like in [8], each flux tube was treated as a 1D RF sheath. Plasma parameters were assumed constant along field lines, and thus only the 2D transverse variation of the density n had to be solved. Parallel losses, turbulent diffusion and RF-induced convection were taken into account, yielding the equation

$$\nabla_{\perp} (n \mathbf{v}_{\perp} - D_{\perp} \nabla_{\perp} n) + n c_s / L_{\parallel} = 0; \quad \mathbf{v}_{\perp} = \frac{\nabla_{\perp} V_{\text{rect}} \times \mathbf{B}}{B^2}; \quad V_{\text{rect}} = 0.4 \left| \int_{\text{fieldline}} \mathbf{E}_{\text{RF}} \cdot d\mathbf{l} \right|$$

In this expression, L_{\parallel} is the length of open field lines, an output of step 2, c_s is the plasma sound velocity, calculated for a temperature of 40eV at the edge, and D_{\perp} is a prescribed anomalous diffusivity of $1\text{m}^2/\text{s}$. As boundary conditions, n was imposed at the plasma side, and was zero at the wall. Convection across boundaries was assumed to vanish. The transport equation was solved by a finite difference method on a 100×100 point mesh. Figure 4 is the resulting density map in a poloidal cross section near the antenna.

Superimposed are two lines representing the bumpers and the FS edge. In spite of the various simplifications of the model, several features seem qualitatively relevant. First, a large density depletion is visible above the antenna, extending to the upper part of the FS. Density is also reduced in front of the straps, with poloidal modulations due to FS bars. Conversely, a large over density sets in under the bumpers, and a smaller one near the FS corner. Figure 5 is a mapping of the parallel RF-induced heat fluxes. It shows poloidal asymmetries with maxima in the lower part of the antenna. Heat fluxes are however less localized than the hot spots on CCD films. They have the right order of magnitude for causing the damages observed on FS.

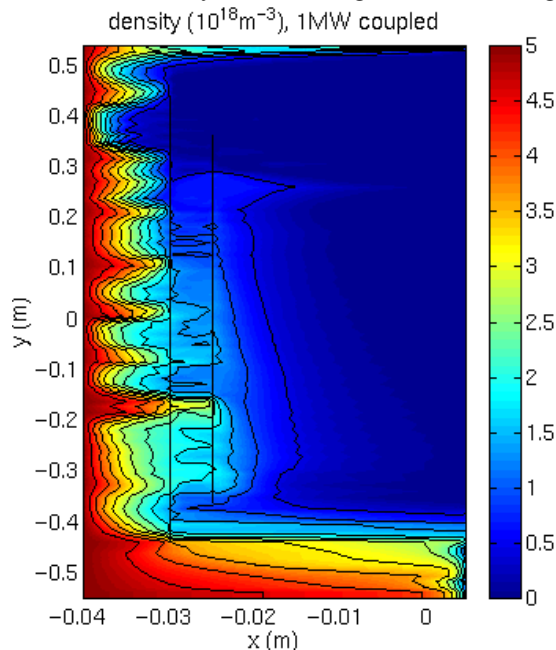


Fig. 4 : density map, dipole phasing.

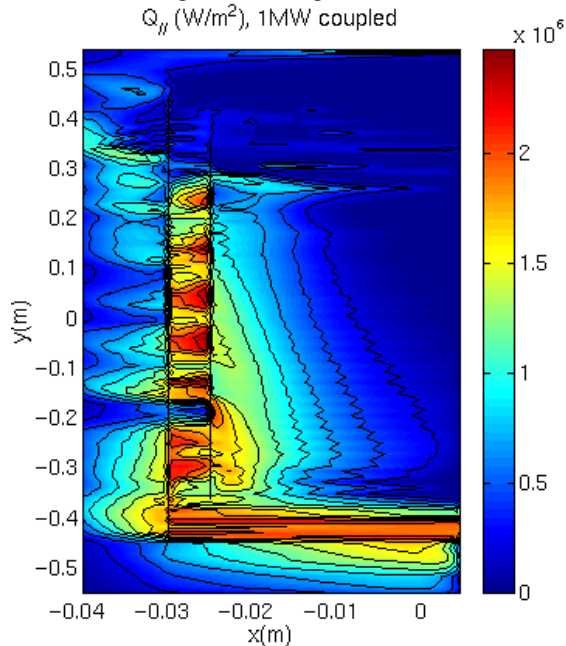


Fig. 5 : parallel RF heat flux map.

3. Conclusions, prospects.

Both experimental and numerical results stress the role of density in the physics of hot spots on ICRF FS. Experimental parametric studies with ED confirm the trends observed in limiter configuration. Apart from the local RF field, they especially identify the overall density near the antenna as a relevant factor for the spurious heating. To explain the heat-load asymmetries on the IR pictures, density redistribution around the antenna by RF-induced $\mathbf{E} \times \mathbf{B}$ transport was put forward. To evaluate these RF-sheath effects in realistic geometry, a set of numerical tools was developed. Simulations validate qualitatively the proposed mechanism, and are in reasonable quantitative agreement with experiments. The codes will be further sophisticated, and used for assessing new Tore Supra antenna designs. It is also planned to test experimentally the presence of density asymmetries in the next plasma campaign, by Langmuir probe measurements near the antenna frame, and through a magnetic field reversal.

References

- [1] : Colas L. & al., *proc. 13th Topical RF conference*, April-1999, Annapolis (USA), 128.
- [2] : Perkins F., *Nucl. Fusion* **29** (1989), 583.
- [3] : Myra J., D'Ippolito D., *Phys. Plasmas* **3** (1996), 699.
- [4] : Meslin B., & al., *proc. 24th EPS Europhysics conf. Abstract*, 21A-I (1997) pp 197-200
- [5] : Thomas C., Harris J., et al, *Fusion Technology* **30** (1996), 1.
- [6] : Hanson G.& al., *Proc. 11th Topical RF Conf.*, Palm Springs, (USA), May, 1995, 463.
- [7] : Pécoul S., S. Heuraux & al, at this conference.
- [8] : Myra J., D'Ippolito D., Ho Y., *Fusion Engineering and Design*, **31** (1996), 291